Tabriz Journal of Electrical Engineering (TJEE), vol. 56, no. 1, 2026 Serial no. 115
DOI: 10.22034/tjee.2026.70715.5110

Design of Ka Band Rotary Joint in Printed Microstrip Gap Waveguide Technology

M. H. Ostvarzadeh Ravari*

Dept. of Elect. & Comp. eng., Graduate University of Advanced Technology, Kerman, Iran
Mh.ostovarzadeh@kgut.ac.ir
*Corresponding author

Received: 23/12/2025, Revised: 14/04/2026, Accepted: 30/05/2026

Abstract
A millimeter-wave rotary joint based on printed microstrip gap waveguide technology is presented. To this goal, a unit cell structure which its bandstop contains the desired frequency band was first designed. The rotary joint structure is proposed as a rectangular cavity surrounded by the designed periodic mushrooms realized on microstrip board and its top layer is a metallic disk placed with an air gap distance from microstrip board. The rectangular cavity is fed by two coaxial ports connected at its both sides. Simulation results show a narrow band insertion loss for designed rotary joint because the cavity is excited at its first mode. To widen its bandwidth, shorting patch and window are introduced in the cavity. The dimensions of the proposed rotary joint were optimized by time domain solver of CST software to obtain the best insertion loss behavior over the desired frequency band. Simulation results show the return loss is better than 10 dB and the insertion loss is less than 0.5 dB over about 21% relative bandwidth. Comparsion of the simulation results with those obtained by freqency domain solver of CST software confirms the accuracy of the design and simulations.

Keywords
Rotary joint, milimeter-wave, printed microstrip, gap waveguide, low loss.

1. Introduction

Rotary joints are key components in radar, satellite, and communication systems, enabling the transmission of microwave/millimeter wave signals between stationary and rotating parts [1]. This module plays a vital role in military, aerospace, and satellite applications, where low-loss, high-stability power and data transfer during rotation are essential. In general, a rotary joint contains rotor, stator, and rotary choke. The stator is connected to the stationary transceiver while the rotating antenna is connected to the rotor part. The rotary choke provides the connection between the rotor and the stator during rotation. With the advancement of modern systems, the design of microwave rotary joints faces challenges such as minimizing insertion loss, improving power handelling capability and bandwidth and enhancing mechanical durability [2].

Rotary joints have been proposed in different planar technologies such as strip line [3] and substrate integrated waveguide technology [4-6]. The main advantages of PCB technologies are their low fabrication cost [7-8], low weight, ease of fabrication and integration with other components, but they suffer from dielectric losses and low power handling capability.

Metallic waveguide rotary joints have the ability to transfer high electromagnetic power with no dielectric loss [9], but they suffer from fabrication complexity and costs.

Recently Gap waveguide technology has been proposed [10-11] especially for millimeter-wave applications that offers low loss components with high power-handling capability and simplified manufacturing process compared to traditional waveguides. Unlike conventional waveguides, which rely on continuous metallic walls to confine electromagnetic waves, gap waveguides utilize periodic structures to create an effective electromagnetic bandgap (EBG) that prevents wave leakage. This unique property eliminates the need of electrical contact between their metal blocks, making them highly suitable for high-frequency applications and multi-layer structurs where mechanical tolerances and assembly precision are critical [12-15].

Rotary joints have been designed in gap waveguide technology thanks to no electrical contact between stationary and rotating part [16-18]. Although GW technology removes complexity of the conventional waveguides, but it suffers from cost and time of CNC drilling process. In this paper, we propose a rotary joint in the printed microstrip gap waveguide technology which is more cost effective and has less time-consuming fabrication process.

2. Printed Ridge Gap Waveguide

2.1. Gap Waveguide Concept

The concept of gap waveguide comes from preventing the propagation of electromagnetic waves in undesired directions and allowing them to propagate in the desired direction [10-11]. According to gap waveguide concept, if the distance of two PEC/PMC parallel plates is less than quarter wavelength, as is shown in Fig. 1, using Maxwell equations and boundary conditions leads to no electromagnetic wave propagation between two parallel plates because all parallel plate modes are in cut off status. This frequency range is called stop band. It is obvious that there is no PMC in nature, therefore these surfaces can be fabricated artificially (Artificial Magnetic Conductor) using periodic pins [11]. By optimizing the period and

dimensions of the pins, the stop band can be designed for the desired frequency band [19].

2.2. *Mushroom Type pins*

In the metallic gap waveguides the pins are fabricated by CNC machining which is time and cost consuming process. The printed ridge gap waveguide is an advanced transmission line technology that combines the benefits of conventional gap waveguides with the simplicity of printed circuit board (PCB) fabrication [20]. This structure consists of a metallic ridge printed on a dielectric substrate, surrounded by a periodic EBG surface, which consists of shorted square or circular patchs that are periodically spaced apart and a metal plate is placed with an air gap distance above them, that prevents wave leakage. In other words, using periodic cells, artificial magnetic conductor surface can be created, which can create a parallel-plate bandgap which suppresses parallel-plate modes, ensuring efficient signal propagation along the ridge. Closed form empirical expressions were also provided for the effective dielectric constant, characteristic impedance, and the dispersion effect of microstrip ridge gap waveguides [21]. Compared to planar technologies, PRGW has the advantage of lower dielectric losses and higher power handling capacity. In comparsion with traditional waveguides, PRGW eliminates the need of electrical contact between top and bottom plate, reducing manufacturing complexity while maintaining excellent wave confinement at microwave and millimeter-wave frequencies and can be integrated with other planar circuits. Compared to metallic GW technologies, PRGW has less complexity and is more cost effective for fabrication and also can be integrated with other planar circuits. For these reasons, recently this technology has gained significant attention for design and manufacturing of microwave componenents and antennas especially at milimeterwave frequencies [22-27].

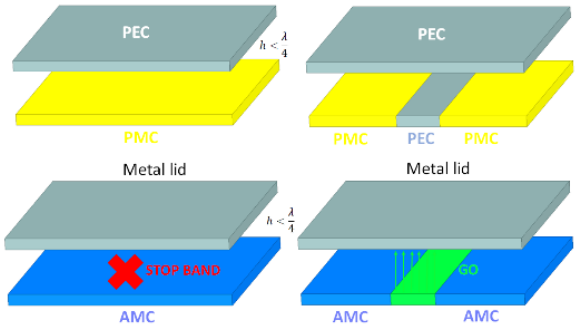

Fig. 1. The concept of gap waveguide technology, green arrow means propagation is allowed, red crosses mean propagation is forbidden.

2.3. *Unit Cell*

The principal step to provide a stopband in a desired frequency range is first determining lower and upper limits of the operating frequency band. Then, the geometric parameters of the air gap and the periodic structure must be optimized to obtain a band gap which its lower and upper limit are defined.

Unit cell which is a shorted metallic circular or rectangular patch like mushroom is a basic building block of the electromagnetic bandgap (EBG) structure in PRGWs, adopted for suppressing unwanted modes and creating a stopband at the desired frequency band.

This paper presents the design of a PRGW unit cell optimized for a stopband centered at 30 GHz, targeting applications in 5G mm-wave systems, satellite communications, and radar. The proposed unit cell leverages a mushroom-type EBG structure printed on a dielectric substrate to achieve strong wave confinement and minimize leakage losses.

Fig. 2 shows a unit cell of the periodic mushroom type EBG surface. A low-loss Rogers RT/Duroid 6002 substrate ($\varepsilon_r = 2.94$, $\tan\delta = 0.0012$) with height 0.762 mm is chosen to minimize dielectric losses at 30 GHz. a circular patch with radius a and thickness t is printed on the substrate which is connected to the ground by a via with radius d. The top metal plate is placed at the height g from the substrate. The length of the unit cell is defined to be $2a+p$ which is the period of mushroom type EBG structure. To adapt the bandgap of periodic mushroom structure in Ka band, the parameters of the unit cell were optimized as is shown in Table I. These parameters were tunned using dispersion analysis of CST software ensuring the bandgap of periodic mushroom structure from 24 GHz to 39 GHz. the dispersion diagram of an infinite periodic structure is shown in Fig. 3. As is clear from Fig. 3, any mode can not propagate in the designed frequency range which is called stopband.

3. Rotary joint design

3.1. *Proposed Structure*

Fig. 4 shows the proposed rotary joint structure which two coaxial lines are considered as its input (bottom) and output (top) ports. The coaxial ports are assumed , 50 ohm, RG 405U cables with Teflon dielectric which are compatible for using at Ka band. The microwave signal transfers from port 1 to 2 through a rectangular cavity which its bottom layer is RT/Duroid 6002 substrate, its top disk is PEC and the side walls are shorted mushrooms, which create a band stop to prevent leakage of electromagnetic waves in the desired frequency band. The bottom layer is the fixed part and the top layer is the rotating part and a distance (air gap) between them allows rotation of top disk. The position and height of coaxial probe are optimized by CST Studio software for the best insertion loss. The final dimensions of the proposed rotary joint are given in Table II.

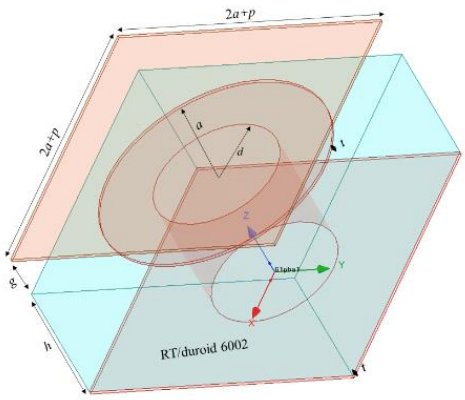

Fig. 2. 3D view of the unit cell.

Table I. Unit cell dimensions.

Parameter	Value (mm)
a	1
d	0.37
g	0.762
h	0.762
p	0.3
t	0.017

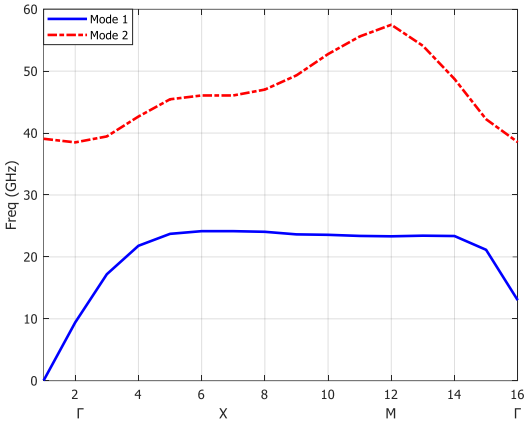

Fig. 3. Dispersion diagram of the periodic pin structure.

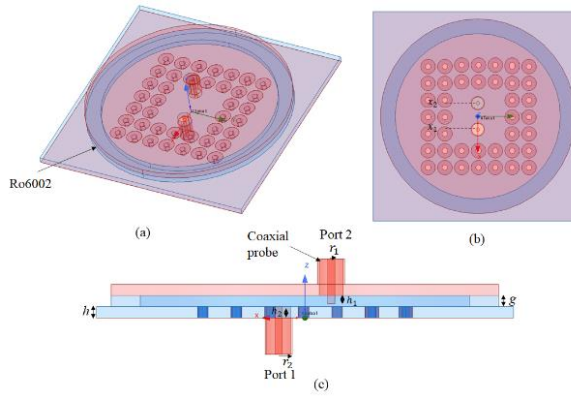

Fig. 4. (a) 3D view (b) top view (c) side view of the proposed rotary joint.

Figs. 5 (a) and (b) shows the return loss and insertion loss of the proposed rotary joint, respectively. As is clear from these figures, the designed rotary joint is a narrow band structure that is because of the resonating mode of the rectangular cavity which allow the cavity to resonate at certain frequency. Fig. 6 shows the magnitude of electric field distribution inside the rotary joint at resonating frequency. As is clear from Fig. 6, the cavity resonates at its first resonant mode. The other point is that the electromagnetic wave does not leak out of the cavity.

Table II. Dimensions of the rotary joint.

Parameter	Value (mm)
r_1	0.255
r_2	0.825
x_1	1.93
x_2	1.8
h_1	0.608
h_2	0.82

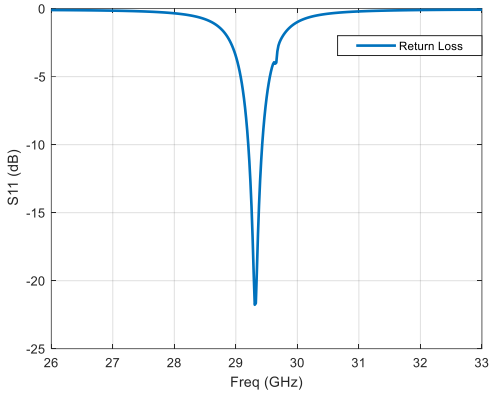

(a)

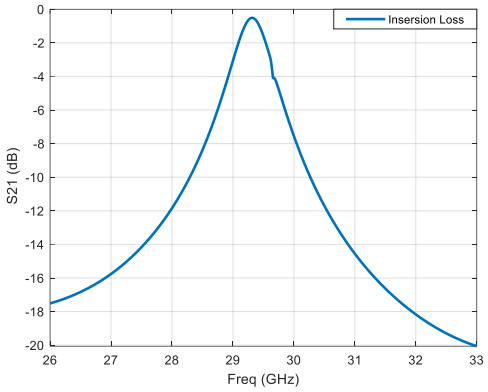

(b)

Fig. 5. Magnitude of (a) Return loss and (b) insersion loss of the designed cavity.

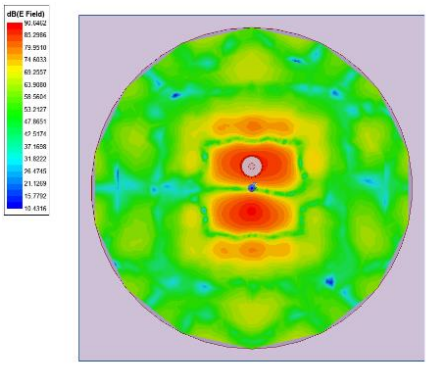

Fig. 6. Magnitude of electric field distribution on the bottom surface of metallic disk @ f=29.3 GHz.

To enhance the bandwidth, a short patch which has a capacitive impedance and a matching window which acts as an inductive impedance have been used [28], as is shown in Fig. 7. These patchs allow the cavity to resonate in wider frequency band. Consequently, a wideband impedance matching can be obtained by tuning the length and width (l_i and w_i, i =1,2) and position ((x_3,0) and (x_4,±y_4)) of the patchs and the position (x_i , i=1,2) and

height (h_i , i=1 to 4) of coaxial probes. These parameters were optimized to have a wide band insertion loss by time domain solver of CST Studio software. The Final dimensions of the structure are presented in Table III.

3.2. *Spacer Application*

A dielectric substrate of thickness g was used in order to hold the rotating disk on the top of the fixed substrate containing mushroom type pins, as is shown in Fig. 8.

3.3. *Moving the Top Plate*

In order for the rotating part to rotate during operation, the upper metal disk must rotate around the center of the coaxial probe attached to it. For this purpose, we consider the upper coaxial probe as the center of the upper metal disk and enlarge the radius of the disk to cover all the shorted mushrooms. The final geometry of the designed rotary joint is shown in Fig. 9.

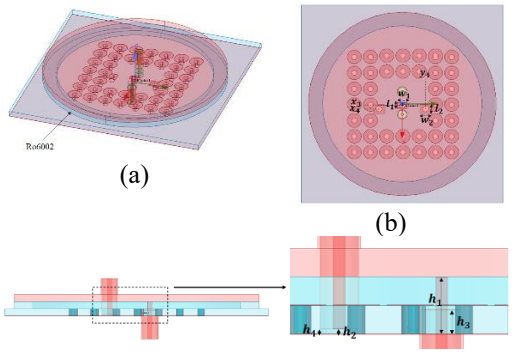

Fig. 7. (a) 3D view(b) top view (c) side view and enlarged side view of the proposed rotary joint.

Table III. Final dimensions of the designed rotary joint.

Parameter	Value(mm)	Parameter	Value (mm)
h_1	1.514	w_1	1.61
h_2	0.142	w_2	1.59
h_3	0.642	x_3	0.083
h_4	0.128	x_4	0.393
l_1	0.85	y_4	-3.27
l_2	1.25		

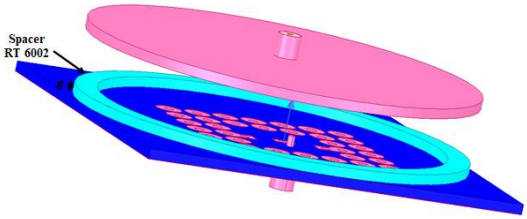

Fig. 8. Applying the spacer to hold the top disk.

4. Simulation results

Fig. 10 (a) shows the logarithmic distribution of magnitude of the electric field distribution in the air gap region between bottom mushroom type cavity and top metal disk when excited from bottom port. As is obvious from this figure, the electric field is concentrated at the middle of cavity and is attenuated sharply on the EBG surface. Also as is shown in Fig. 10 (b) the electromagnetic energy is transferred to the top coaxial probe through the air gap, when the rotary joint is excited from bottom coaxial probe.

The *S*-parameters of the optimized rotary joint are shown in Fig. 11. As is seen from this figure, the return loss is better than 10 dB in 26.2-32.6 GHz frequency band. According to Fig. 11(b), the magnitude of S_{21} is better than -0.5 dB over the desired frequency band which shows about 21% relative bandwidth. Simulations were performed by TD solver of CST software. To validate the results, simulasion were repeated by FD solver of CST software. Comparsion of the simulation results, which obtained by both TD an FD solvers, confirms the accuracy of the simulations as is shown in Fig. 11

Simulations were repeated considering 0.01 mm tolerance for important parameters of the rotary joint simutaneously. It was seen that the insersion loss was better than 0.5 dB over the desired frequency band in all of the predicted scenarios.

The comparsion between the proposed rotary joint and previous works is shown in table IV. As is clear from this table, the proposed rotary joint is cost effective for fabrication although its relative bandwidth is small due to the low pin height and low air gap thickness.

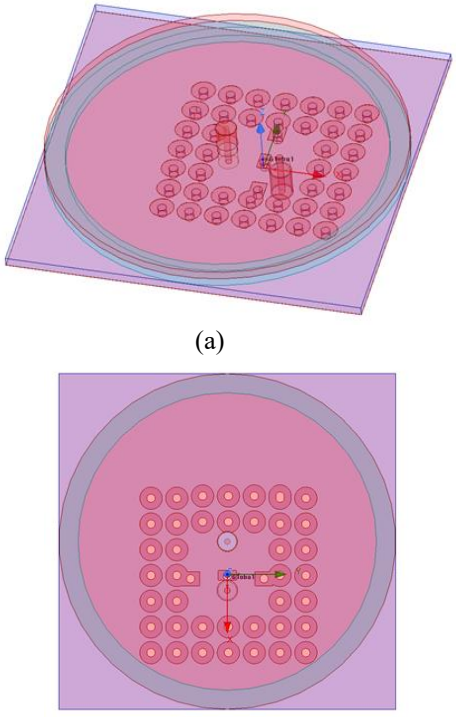

Fig. 9. (a) 3D view(b) top view of the rotary joint.

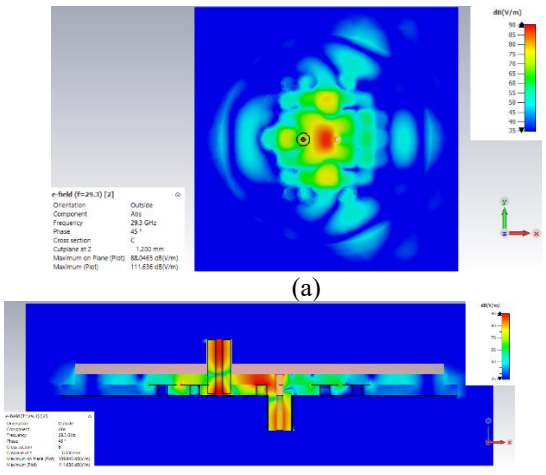

(a)

(b)

Fig. 10. Electric field distribution in the rotary joint (a) top view (b) side view.

5. Conclusion

In this work, a planar low loss rotary joint was designed in printed microstrip gap waveguide technology. For this purpose, a substrate containing mushroom-shaped pins, which designed to work at the desired frequency band, was considered as the fixed part and a rotating metal disk was placed at a small height above it. Two coaxial probes were considered as the ports of this structure. The dimensions of the proposed rotary joint were optimized to obtain widest bandwidth.

The benefit of the PRGW vs. GW technology is that it does not need CNC drilling, therefore it is easy and cost effective to manufacture due to using PCB technology. But the bandwidth of the proposed rotary joint is confined because the height of pins can not be changed and the air gap thickness is limited. Further works can be bandwidth enhancement techniques using multilayer PCB boards or multi-cavity rotary joint structure realized in PRGW technology and using waveguide ports to increse power handling capability.

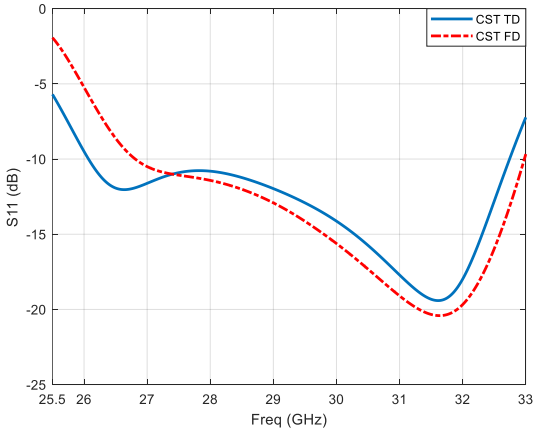

(a)

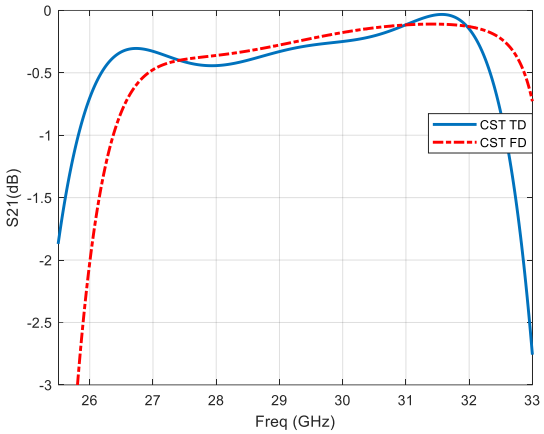

(b)

Fig. 11. Magnitude of (a) Return loss and (b) insersion loss of the final optimized rotary joint.

Table IV. Performance comparison among several rotary joints.

Ref.	BW/f_0 (%)	$I.L$ (dB)	Power handling /loss	Cost
[3]	N.A	0.3	Low/High	Low
[4]	9.1	≤ 1.09	Low/High	Low
[9]	4.5	≤ 0.8	High/Low	High
[16]	55	≤ 0.28	High/Low	Medium
This work	21	≤ 0.5	High/Low	Low

6. References

[1] S. Borisov and A. Shishlov, “Antennas for Satcom-on-the-move, review,” in Proc. Int. Conf. Eng. Telecommun., Nov. 2014, Moscow, Russia, pp. 3–7.

[2] D. Haas, M. Thumm, J. Jelonnek , “Broadband Rotary Joint Concept for High-Power Radar Applications”, *Journal of Infrared, Millimeter, and Terahertz Waves*, vol. 42, pp. 107–116, 2021.

[3] E. D. Evans, “An analysis of a coupled-ring rotary joint design,” *IEEE Transactions on Microwave Theory and Techniques*, vol. 40, no. 3, pp. 577–581, 1992.

[4] Y. Jian Cheng, Z. J. Xuan, “12-GHz Rotary Joint With Substrate Integrated Waveguide Feeder”, *IEEE Transactions on Microwave Theory and Techniques* vol. 64, iss. 5, pp. 1508-1514, 2016.

[5] Z. J. Xuan and Y. J. Cheng, “Rotary joint perpendicularly fed by a substrate integrated waveguide feeder,” *IEEE Transactions on Microwave Theory and Techniques*, vol. 65, no. 10, pp. 3761–3768, 2017.

[6] L. Zhao, J. Shi, and K. Xu, “Broadband coaxial rotary joint with simple substrate integrated waveguide feeder,” *IEEE Access*, vol. 7, pp. 139499–139503, 2019.

[۷] محمد سجاد بیاتی، تحسین خورند، «طراحی و ساخت مجیک‌تی یک لایه با استفاده از موجبر نصف مد مجتمع‌شده در زیرلایه برای کاربردهای باند Ku»، *نشریه مهندسی برق تبریز*، دوره ۴۹، شماره ۱، ۲۳۵-۲۴۰، ۱۳۹۸.

[۸] حبیب قربانی نژاد فومنی، امید اتحاد محکم، «طراحی، تحلیل و شبیه-سازی یک فیلتنای مایکرواستریپ با روی‌کرد طراحی فیلتر میان‌گذر»، *نشریه مهندسی برق تبریز*، دوره ۴۹، شماره ۲، ۷۹۱-۷۸۳، ۱۳۹۸.

[9] A. Yevdokymov, V. Kryzhanovskiy, V. Pazynin, K. Sirenko, “Ka-band waveguide rotary joint”, *IET*

Microwaves, Antennas & Propagation, vol. 7, Iss. 5, pp. 365-369, 2013.
[10] P.-S. Kildal, E. Alfonso, A. Valero-Nogueira, and E. Rajo-Iglesias, "Local Metamaterial-Based Waveguides in Gaps Between Parallel Metal Plates," *IEEE Antennas and Wireless Propagation Letters*, vol. 8, pp. 84–87, 2009.
[11] P.-S., Kildal, "Artificially soft and hard surfaces in electromagnetics," *IEEE Transactions on Antennas and Propagation*, vol. 38, pp.1537-1544, 1990.
[12] A. U. Zaman and P.-S. Kildal, "Gap Waveguide for Packaging of Microwave Components," *IEEE Transactions on Microwave Theory and Techniques*, vol. 62, no. 10, pp. 2263–2272, 2014.
[13] M. H. Ostovarzadeh, S. A. Razavi Parizi, "Design of Ku Band Monopulse Antenna in Gap WaveguideTechnology," *journal of Radar*, vol. 8, no. 1, pp.111-117, 2020 (in persian).
[14] R. Askarzadeh, A. Farahbakhsh, Davood Zarifi, A. Uz Zaman, "Wideband High-Efficiency Slot Array Antenna Based on Gap Waveguide Single-Layer Feeding Network " *IEEE Antennas and Wireless Propagation Letters*, Vol. 24, Iss. 2, pp. 519-523, 2025.
[15] A. Farahbakhsh, D. Zarifi, A. Vosoogh, ,Carlo Bencivenni, Michal Mrozowski, " A Wideband 8 × 8 Slot Array Antenna Using Gap Waveguide MLW Coaxial Line Technology for mmWave Applications*," IEEE Antennas and Wireless Propagation Letters*, vol. 24, Iss. 7, pp. 1974 – 1978, 2025.
[16] A. Farahbakhsh, "Wideband Rotary Joint Based on Gap Waveguide Technology" *IEEE Transactions on Microwave Theory and Techniques* , vol. 69, no. 10, pp. 4385-4391, 2021.
[17] A. Farahbakhsh, D. Zarifi, M. Mrozowski, "Design of mmWave Broadband Rotary Joint and 360° Beam-Steering Rotenna Based on Gap Waveguide Technology," *IEEE Transactions on Antennas and Propagation*, vol. 73, Iss. 7, pp. 4373 – 4383, 2025.
[18] M. Nasri, D. Zarifi, "Design and Simulation of Waveguide Rotary Joint Based on Gap Waveguide Technology for 60 GHz Applications" *Journal of Radar*, vol. 8, no. 2, (serial no. 24), pp. 73-78, 2021 (in persian).
[19] E. Rajo-Iglesias and P.-S. Kildal, "Numerical studies of bandwidth of parallel-plate cut-off realized by a bed of nails, corrugations and mushroom-type electromagnetic bandgap for use in gap waveguides," *IET Microwaves Antennas Propagion*. vol. 5, no. 3, pp. 282-289, Feb. 2011.
[20] H. Raza, J. Yang, P.-S. Kildal, E. Alfonso, "Microstrip-Ridge Gap Waveguide-Study of Losses, Bends and Transition to WR-15," *IEEE transactions on microwave theory and techniques*, vol. 62, no. 9, pp. 1943- 1952, 2014.
[21] A. T. Hassan; M. A. M. Hassan; A. A. Kishk, "Modeling and Design Empirical Formulas of Microstrip Ridge Gap Waveguide," *IEEE Access*, vol. 6, pp. 51002-51010, 2018.
[22] X. Hu and X. Feng, "Ka-band coupled-resonator bandpass filter based on printed ridge gap waveguide for millimetre‐wave application*," Electronics Letters*, vol. 57. no. 20, pp. 770-772, 2021.
[23] T. Zhang, L. Chen, A. U. Zaman, and J. Yang. "Ultra-wideband millimeter-wave planar array antenna with an upside-down structure of printed ridge gap waveguide for stable performance and high antenna efficiency", *IEEE Antennas and Wireless Propagation Letters*, vol. 20, no. 9 pp. 1721-1725, 2021.
[24] M. M. Ali, et al. "Ultra-wideband compact millimeter-wave printed ridge gap waveguide directional couplers for 5G applications", *IEEE Access*, vol. 10. pp. 90706-90714, 2022.
[25] M. O. Shady and A. M. M. A. Allam, "A novel design of printed ridge gap waveguide-based 0 dB backward wave coupler, *International Journal of RF and Microwave Computer-Aided Engineering*, vol. 32. no. 11, p.e. 23386, 2022.
[26] Y. Al-Alem, et al. "Circularly polarized ka-band high-gain antenna using printed ridge gap waveguide and 3-D-printing technology," *IEEE Transactions on Antennas and Propagation*, vol. 71. No. 9 pp. 7644-7649, 2023.
[27] M. Taraji, E. Baladi, and Marco A. Antoniades. "Compact wideband and high gain horn slot antenna array fed by printed ridge gap waveguide for X band applications", *Scientific Reports*, vol. 15, no.1, pp. 17627, 2025.
[28] N. Marcuvitz, "Waveguide Handbook", MIT Radiation Laboratory Series, vol. 10. New York, McGraw-Hill, 1948.